Fractal Analysis of Polypropylene Composite Filled with Nano-Calcium Carbonate

Shaoyan Yuan, Hong Xu, Hongchen Gu

National Key Laboratory of Nano/Micro Fabrication Technology, Research Institute of Micro/Nano Science and Technology, Shanghai Jiaotong University, Shanghai 200030, China

Received 4 April 2006; accepted 30 July 2007
DOI 10.1002/app.27718
Published online 7 August 2008 in Wiley InterScience (www.interscience.wiley.com).

ABSTRACT: Polypropylene (PP) and nano-calcium carbonate ($CaCO_3$) composites were prepared by melt mixing in a corotating twin-screw extruder. Transmission electron microscopy study and particle size analysis revealed the dispersion and the size distribution of $CaCO_3$ in PP. With the increase of loading of filler, $CaCO_3$ nanoparticles densely aggregated together and the dispersion of filler became bad. The fractal dimensions of the composites were determined using fractal concept. The fractal dimensions of D and D_k described the irregularities of the shape of an object and the distributions of particle populations, respectively. The D and D_k values were influenced by the content of filler, i.e., the D values increased, and the D_k values decreased with the increase of loading of filler. When the loading of filler was low, the values of D and D_k of PP composites differ slightly than the counterparts of PP/PP-*g*-MA (50 wt %) blend. For 20 wt %, they were almost identical. This fact showed that the fractal dimension was correlated with the dispersion. © 2008 Wiley Periodicals, Inc. J Appl Polym Sci 110: 1955–1960, 2008

Key words: polypropylene; calcium carbonate; dispersion; fractal dimension

INTRODUCTION

The nanoparticles, such as montmorillonite, silica,[1] and calcium carbonate ($CaCO_3$),[2] have been used to prepare nanocomposites because they could provide surface smoothness and high gloss compared with micron-sized ones[3] and have an advantage in the application to film and fiber.[4,5] Among them, $CaCO_3$ is one of the most commonly used inorganic fillers for thermoplastics, because of the high quality/cost ratio, such as poly(vinyl chloride), polypropylene (PP), polystyrene.[6]

As we know, nanosized filler, if well dispersed in polymer matrix, may significantly augment the properties of composites. Unfortunately, the filler particles tend to aggregate during processing, resulting in aggregates and agglomerates. The objective of dispersion is to reduce these aggregates and agglomerates to an acceptable size. Therefore, filler dispersion is an important parameter to obtain a homogeneous finished compound and improve the performance.

Correspondence to: H. Xu (xuhong@sjtu.edu.cn).

Contract grant sponsor: Shanghai Natural Science Foundation of China; contract grant number: 04ZR14086.
Contract grant sponsor: Shanghai Nano Technology Project of China; contract grant number: 0352nm023.
Contract grant sponsor: Zhejiang Gongguan Project; contract grant number: 2004C11019.

Filler dispersion is commonly characterized by particle size and its distribution. Particle size distribution data are typically presented graphically on a grain size-distribution plot. Numerical quantities such as the uniformity coefficient and the coefficient of curvature are used to add further descriptive refinement; however, quantification of particle size distribution by only considering a few points, or a limited portion, along the grain size distribution curve has inherent limitations. Fractal fragmentation theory provides a means by which the entire size distribution of material can be quantified.[7]

Fractal analysis has become a new and powerful tool to describe the geometric and structural properties of fractal surfaces, particle boundaries, and pore structures, since their complex patterns are better described in terms of fractal geometry as long as the requirement of self-similarity is satisfied.[8] The latter term implies that the geometrical features of an object are independent of the magnification or observation scale.[9] Fractal dimensions have been used to quantify the morphology of individual particles since the late 1970s.[10] An early application of fractal dimensions to describe particle form in the geosciences was discussed by Orford and Whalley[11] who found that many particles had Richardson plots displaying two or three linear segments. They used the terms ''textural fractal'' and ''structural fractal'' to refer to aspects of particle form resulting from the microscale surface texture of the particle and the

larger scale, overall shape, respectively. Kaye[12] discussed alternative methods (e.g., box counting, dilation) of determining the fractal dimension of individual particles.

In this work, the $CaCO_3$ nanoparticles filled PP was used as a model compound. The morphology and dispersion of $CaCO_3$ nanoparticles dispersed in PP composites were analyzed. Employing the fractal concept, the particle size and its distribution were characterized by means of perimeter–area relationships and Korcak's empirical law.[13] The main objective of this article was to report on the fractal nature of these features and to correlate them with the dispersion of nano-$CaCO_3$ filled polymer.

METHODS

Theoretical background

Collections of similar objects have been found to have area–perimeter relationships described by a power function

$$P \propto A^{D/2} \tag{1}$$

where P is the perimeter, A is the projected area, and D is the fractal dimension of the object. For Euclidean objects, $D = 1$. $D > 1$ has been found for fractal objects, such as individual flocs in streams.[10] Consequently, as the object area becomes larger, the perimeter increases more rapidly than for Euclidean object, which indicates that the boundary of the objects is becoming more convoluted.

Distributions of particle populations can be described using Korcak's empirical law

$$N(a > A) \propto A^{-D_k/2} \tag{2}$$

where N $(a > A)$ is the rank or the number of an object with an area (a) greater than a certain area (A) and D_k is the fractal dimension that describes the total object area over small and large objects.[13] The fractal dimension D_k is calculated as minus two times the slope of the regression line between projected area and particle rank.[14] Many size distributions in nature follow Korcak's empirical law, including the fragmentation of rock into smaller and smaller sizes.[15]

Materials

PP homopolymer (T300; Sinopec, China) having melting flow index of 3.0 g/10 min (2.16 kg at 230°C), Maleic anhydride grafted PP (PP-*g*-MA; Guangzhou Kingfa Science and Technology, China) with 1 wt % grafting percentage of MAH, $CaCO_3$ with average particle size of 0.05 μm, and stearic acid used to modify the surface to improve the affinity between the $CaCO_3$ nanoparticles and the polymer (Shanghai Yaohua Nano Technology, China) were used in this experiment.

Specimen preparation

The dispersion of a filler in a polymer is better with a twin-screw extruder than with a single-screw extruder or a Banbury mixer. In this study, compounding of the materials was done using an o-rotating twin-screw extruder (TE-35; Jiangsu Keya, China). The L/D ratio of the screws was 38, and D = 35 mm. Barrel temperatures of extruder were set at 175/190/200/200/200°C and die temperature was set at 190°C, and a screw speed of 120 rpm was used. After compounding, the pellets of compounds were injection molded into rectangular bars (74 mm × 10 mm × 4 mm) using an injection molding machine. The barrel of the injection molding machine had a flat temperature profile of 210°C, and the mold temperature was kept at 40°C with an injection pressure of 5 MPa.

Characterization of the nanocomposites

The composites were ultrathin sectioned using a microtome equipped with a diamond cutter. The sections (about 70 nm) were mounted on 200-mesh copper grids and dried in a desiccator for more than 24 h before transmission electron microscopy (TEM) examination. The TEM examination of the ultrathin section was conducted on a TEM (JOEL-100) operated at an accelerating voltage of 80 kV.

Image analysis

To test the fractal character of a complex agglomerate structure of filler, the TEM micrographs were taken at different magnifications. The TEM micrographs were digitized into gray images and treated by an image analyzer program (Global Lab Image 3.1). Before processing a particular image, image thresholding was applied, where pixels were classified into two categories, either background or particle. This step effectively filtered out random noise, as well as particles that were not well focused. The overall image was rendered binary, where particles with sharp edges were identified and separated from the background. To extract the greatest amount of information, this step requires good quality images with the least distortion of the edge of the particles.[16] The fractal dimension (D and D_k) was then deduced from the Richardson plots for each of them. To obtain accurate results, two micrographs were considered for each magnification. The perimeter P was obtained by the length (total number of

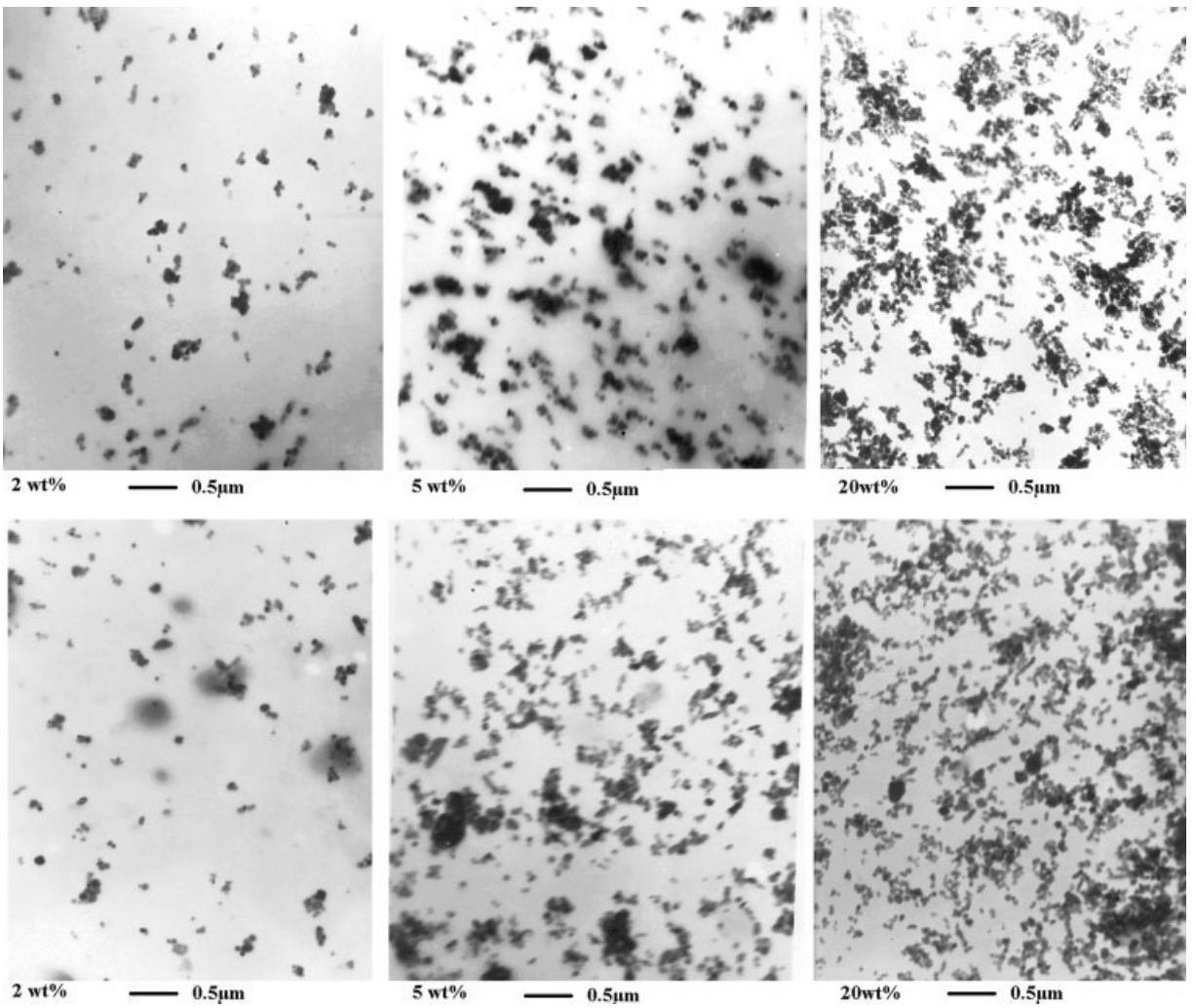

Figure 1 TEM photograph of the PP (top) and PP/PP-*g*-MA (50 wt %) blend (bottom) nanocomposites.

pixels) around the coastline and the area A was obtained by the number of pixels inside its boundary. Mean particle diameter was diameter of a circle of the same area taken up by a particle or aggregate as observed on TEM. The fractal dimension (D) was calculated from the slopes of regression lines on

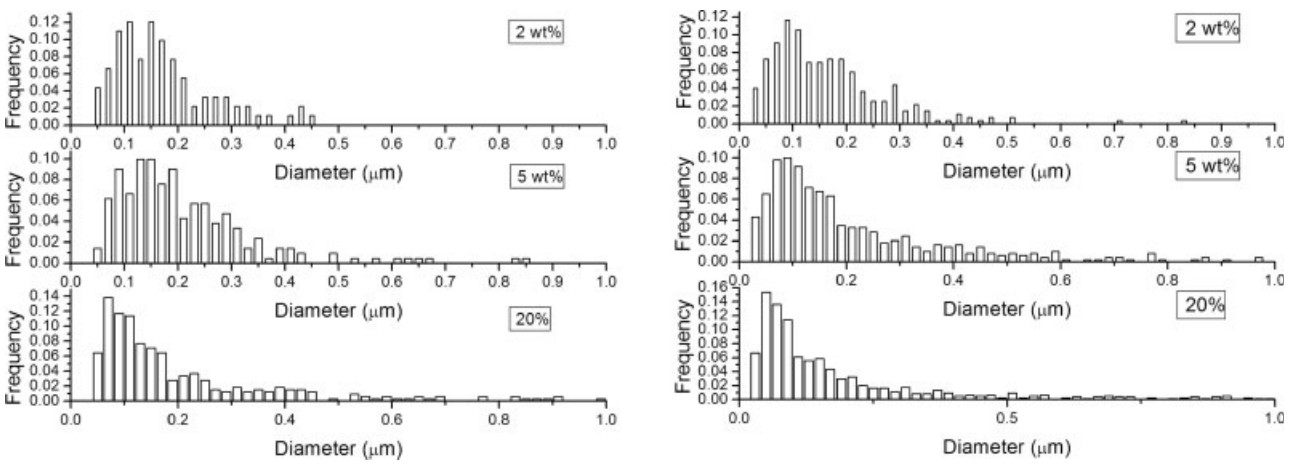

Figure 2 Histograms of size distribution of nano-$CaCO_3$ in terms of diameter in PP (left) and PP/PP-*g*-MA (50 wt %) (right).

TABLE I
Statistics of Particle Size Based on TEM Micrographs

Samples	PP	PP	PP	PP/PP-*g*-MA (50 wt %)	PP/PP-*g*-MA (50 wt %)	PP/PP-*g*-MA (50 wt %)
Contents of filler (wt %)	2	5	20	2	5	20
Mean particle diameter (μm)	0.15	0.17	0.20	0.14	0.16	0.21

log P – log A plots for a minimum of 100 particles per sample, and the D_k was calculated as minus two times the slope of the regression line between particle area and frequency.

RESULTS AND DISCUSSION

Dispersion of filler in PP and PP/PP-*g*-MA (50 wt %) blend

The size distribution for 2 wt % composites (PP and PP/PP-*g*-MA, 50 wt %) is quite narrow (Figs. 1 and 2), and many particles are single particle or aggregates with diameter less than 0.2 μm (Table I). With the increase of the loading of $CaCO_3$, the number and the diameter of the aggregates become large. The results for 20 wt % samples demonstrate the typical tailing toward maximum values of the $CaCO_3$ particle diameter. This implies that the size distribution for the higher loading of $CaCO_3$ particles is quite broad.

The particle dispersion and reagglomeration happen simultaneously during compounding of the polymer composites. The breakup of agglomerates occurs when hydrodynamic forces induced by the melt flow overcome the cohesion forces of the agglomerates; and particle reagglomeration occurs when aggregates are brought together by the nonhomogeneous flow field.[16] Therefore, in general, the higher the loading of $CaCO_3$, the more seriously the filler aggregates.

Fractal dimension of particle by the area-perimeter method

The log P – log A plots for these composites yield straight lines, as shown in Figure 3. The values of D (Table II) are in all cases higher than 1, indicating the fractal nature of the aggregates of filler in PP and PP/PP-*g*-MA (50 wt %). In addition, it is observed that D values increase with the increase of loading of filler for two types of composites. The change in D represents a change in the particle shape as a function of loading of filler and is interpreted as an increase in shape irregularity of larger particles compared to smaller particles. With the increase of loading of filler, the size and number of aggregates increase, and therefore, D increases. In other words, the area of particle population increases but the perimeter increases more rapidly than for Euclidean objects indicating that particle boundaries become more irregular with increasing loading.

Fractal dimension of size distribution of particle

The D_k for each grain size distribution was obtained by first developing a log N versus log A plot and then determining the slope of the best-fit line through the data points using linear regression. The

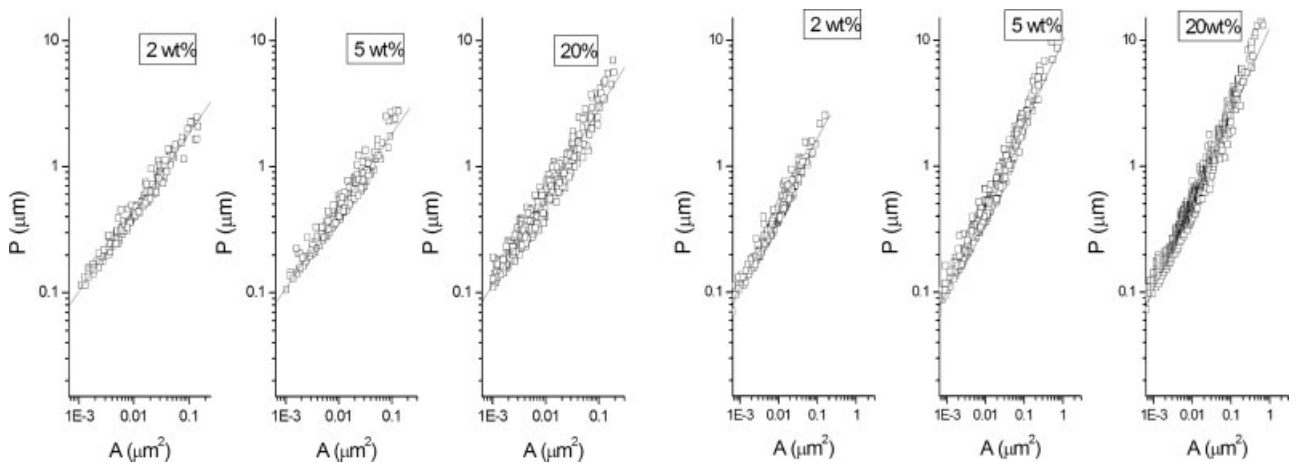

Figure 3 The log P – log A plots for PP (left) and PP/PP-*g*-MA (50 wt %) (right).

TABLE II
Fractal Dimension (D, D_k) of Filler Particle in PP and PP/PP-*g*-MA (50 wt %)

Samples	PP	PP	PP	PP/PP-*g*-MA (50 wt %)	PP/PP-*g*-MA (50 wt %)	PP/PP-*g*-MA (50 wt %)
Contents of filler (wt %)	2	5	20	2	5	20
D	1.22	1.23	1.39	1.2	1.32	1.39
D_k	3.92	3.44	3.34	4.16	3.26	3.24

data from the grain size distribution test results plot as relatively straight lines (Fig. 4) on the plot,[17–22] and therefore it is concluded that fractal theory was applicable. The fractal dimension results for the grain-size distribution tests are summarized in Table II. With the increase of loading of filler, the D_k values of PP and PP/PP-*g*-MA (50 wt %) composites decrease (Table II). D_k is not a measure of the irregularity of the pattern, but a measure of the size number relationship of the population, or in other terms, the fragmentation of the population. Small values of D_k indicate that most of the total object area is concentrated into a smaller number of large objects, whereas large values indicate a more equal size distribution over the entire size range of the particles.[14]

The effective mixing requires not only dispersive mixing to break up agglomerates, but also distributive mixing to promote wetting and minimize agglomeration after filler breakup. The $CaCO_3$ particles are generally supplied as agglomerates, and during processing these aggregates have to be broken up and dispersed into the primary particles. However, large interactions between particles result in inhomogeneous distribution of the filler, processing problems, poor appearance, and inferior properties. The two major factors which determine the particle–particle interactions are particle size and surface free energy. The effects of aggregates on the properties of composites are clearly detrimental. Many authors emphasize this fact together with the importance of best possible homogeneity.[23] The objective of the use of PP-*g*-MA is to improve the compatibility between PP and $CaCO_3$ particles. Therefore, better dispersion of $CaCO_3$ particles in PP/PP-*g*-MA (50 wt %) is expected. As seen in Table I and Figure 2, however, the mean particle diameter for PP/PP-*g*-MA (50 wt %) composite differs slightly than PP. When the loading of filler is low (2 wt %, 5 wt %), the values of D and D_k of PP composites differ slightly than the counterparts of PP/PP-*g*-MA (50 wt %). For 20 wt %, they are almost identical. This implies that the loading of filler is a dominant effect on the dispersion of filler in PP composite.

Fractal dimensions not only reflect the nature of particles and their mechanism of formation,[24] but also reflect the dispersion and morphology of particles dispersed in polymer. Composites properties, such as optical and mechanical properties, are influenced by the dispersion of filler. As a result, the fractal dimension is expected to influence composites properties. The correlation between fractal dimension and composites properties will be reported later.

CONCLUSIONS

The TEM study and histograms of size distribution showed that the nanoparticles were distributed in

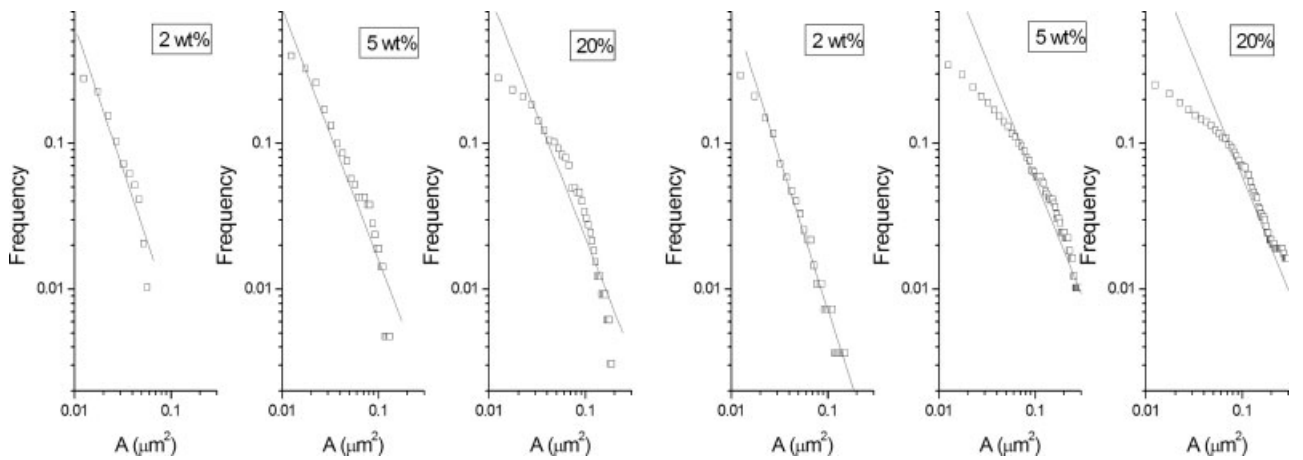

Figure 4 The area distribution of filler particle in PP (left) and PP/PP-*g*-MA (50 wt %) (right).

the PP uniformly and little particle agglomeration was found at 2 wt %. With the increase of filler content, the mean particle diameter increases and the distribution becomes broad. In general, the more complex morphology will exhibit higher fractal dimension. The D results of the PP composites increase with the loading of $CaCO_3$. As a result, the morphology of particles is complicated with the increase of loading of filler. The values of D_k of the PP composites decrease with the loading of $CaCO_3$. Higher fractal dimension (D_k) suggests a higher frequency of smaller features relative to larger features than does a lower fractal dimension.[25] With the increase of loading of filler, particles aggregate together and the dispersion of filler becomes bad. When the loading of filler is low, the values of D and D_k of PP composites differ slightly than the counterparts of PP/PP-*g*-MA (50 wt %). For 20 wt %, they are almost identical. This implies that the loading of filler is a dominant effect on the dispersion of filler in PP composite. Consequently, the fractal dimension is correlated with the dispersion of filler.

References

1. Petrovic, Z. S.; Javni, I.; Waddon, A.; Banhegi, G. J Appl Polym Sci 2000, 76, 133.
2. Rong, M. Z.; Zhang, M. Q.; Zheng, Y. X.; Zeng, H. M.; Walter, R.; Friedrich, K. Polymer 2001, 42, 167.
3. Chan, C.-M.; Wu, J.; Lia, J.-X.; Cheung, Y.-K. Polymer 2002, 43, 2981.
4. Cho, J. W.; Paul, D. R. Polymer 2001, 42, 1083.
5. Rong, M. Z.; Zhang, M. Q.; Zheng, Y. X.; Zeng, H. M.; Friedrich, K. Polymer 2001, 42, 3301.
6. Yuan, S.; Lu, J.; Luo, Y.; Huang, R. Acta Mater Compos Sin 2005, 22, 25.
7. James, P. H.; Luis E. V. Eng Geol 1997, 48, 231.
8. Miller, S.; Reifenberger, R. J Vacuum Sci Technol B 1992, 10, 1203.
9. Lee, S.-B.; Pyun, S.-I. J Electroanal Chem 2003, 556, 75.
10. De Boer, D. H.; Stone, M.; Levesque, M. J. Hydrol Process 2000, 14, 653.
11. Orford, J. D.; Whalley, W. B. Sedimentology 1983, 30, 655.
12. Kaye, B. H. In The Fractal Approach to Heterogeneous Chemistry; Avnir, D., Ed.; Wiley: Chichester, 1989; p 55.
13. Mandelbrot, B. B. The Fractal Geometry of Nature; W.H. Freeman and Company: New York, 1983.
14. Stone, M.; Krishnappan, B. G. Water Res 2003, 37, 2739.
15. Turcotte, D. L. Fractals and Chaos in Geology and Geophysics; Cambridge University Press: New York, 1992; p 95.
16. Miller, B. V.; Lines, R. W. CRC Crit Rev Anal Chem 1988, 20, 75.
17. Barton, C. A.; Zoback, M. D. J Geophys Res 1992, 97, 5181.
18. Mace, R. E.; Marrett, R. A.; Hovorka, S. D. In Proceedings of the 10th Multidisciplinary Conference, San Antonio, TX, 2005; Geotechnical Special Publication, no. 144, pp 178–187.
19. Pfeifer, P. Appl Surf Sci 1984, 18, 146.
20. Pfeifer, P.; Avnir, D.; Farin, D. J Stat Phys 1984, 36, 699.
21. Vstovskii, G. V.; Kolmakov, L. G.; Terent'ev, V. F. Metally 1993, 4, 164.
22. Kozlov, G. V.; Beloshenko, V. A.; Mikitaev, A. K. Mater Sci 2002, 38, 458.
23. Zuiderduin, W. C. J.; Westzaan, C.; Huétink, J.; Gaymans, R. J. Polymer 2003, 44, 261.
24. Meakin, P. The Fractal Approach to Heterogeneous Chemistry; Avnir, D., Ed.; Wiley: Chichester, 1989; p 131.
25. Robert, E. M.; Randall, A. M.; Susan, D. H. Geotech Spec Publ 2005, 144, 178.